

A Novel Biomimetic Wing Design and Optimizing Aerodynamic Performance

Metin Uzun^{1*}, Mustafa Özdemir², Çağrı Vakkas Yıldırım³ and Sezer Çoban³

^{1*} İskenderun Technical University, Department of Airframe and Powerplant Maintenance, 31200, İskenderun, Hatay, Turkey. (metin.uzun@iste.edu.tr).

² Firat University, Aircraft Airframe and Powerplant Department, Elazığ, Turkey. (m.ozdemir@firat.edu.tr).

³ Erciyes University, Aircraft Airframe and Powerplant Department, Kayseri, Turkey. (cvyildirim@erciyes.edu.tr).

⁴ İskenderun Technical University, Department of Airframe and Powerplant Maintenance, 31200, İskenderun, Hatay, Turkey. (sezer.coban@iste.edu.tr).

Article Info

Received: Dec., 18. 2021

Revised: Feb., 15. 2022

Accepted: March, 04. 2022

Keywords:

Aerodynamic

Airfoil

Biomimetic

Wind Tunnel

Wing Design

Corresponding Author: Metin Uzun

RESEARCH ARTICLE

DOI: <https://doi.org/10.30518/jav.11031989>

Abstract

In this article, numerical and experimental analyzes were made by adding winglet and endless blade to the tip of the airfoil to improve the wind turbine blade performance. Similarly, the change in performance was investigated by making notches at different sizes and distances on the trailing edge of the wing structure, inspired by the creatures in nature. First of all, the designed wing structures were analyzed by numerical analysis as a fixed wing, and the lift and drag forces were examined and the aerodynamic performance parameters were examined. Then, the winglet, endless wing and trailing edge notch were mounted to the wing structure cast from a 3D printer, and the energy parameters produced by each design in the wind tunnel were examined. In curved wings, the stress values produced depending on the size of the endless wing structure added to the wing tip have changed and up to 15% aerodynamic performance improvement has been observed in the designed wing structure. In addition, the design was experimentally examined on conventional fixed blades, and up to 6% improvement was observed on fixed blades.

1. Introduction

Increasing world population and technological developments have brought along the increasing energy demand. These developments have accelerated the depletion cycle of non-renewable fossil fuels and have led human beings to seek new energy sources. With the steps taken to produce energy from renewable energy sources, sustainable energy has taken its place among the future energy plans of developed countries and has gained importance (Yılmaz & Kalkan, 2017). Scientists have done many studies in order to take the place of sustainable energy sources in our lives and to spread the use of renewable energy sources to all areas. In these studies, solar cells were developed to benefit from solar energy, and projects such as the use of wind turbines to benefit from wind energy were developed. Today, in order to form the basis of energy policies, it is necessary to diversify existing energy sources and make these sources available (Külekcı, 2009). All of the energy needed on earth comes from the sun, and an average of 2% of this energy is wind energy. The earth's atmosphere warms up at different rates as the sun's rays are absorbed at different rates by plants, water, soil and rocks. Variable pressure zones formed during this thermal exchange are the main driving force of air movement (Johnson, 1985). The heated air mass starts to move from high pressure points to low pressure points and as a result of this mass

displacement, wind formation occurs (Kalmikov, 2017). The kinetic energy of the air mass that creates the winds and displaces due to the pressure difference is called wind energy. In other words, we can call the solar energy converted into kinetic energy as wind energy. The power of the winds increases with the cube of their speed, and their speed increases in proportion to the height (Özkaya et. al., 2019).

Among the obstacles to global energy use forecasts and planned developments such as cost, farm area and technological constraints, the most important is the design of turbine blades, which are in contact with the wind and are the protagonists of electricity generation. Nature, which contains many problems and solutions, has been a source of inspiration for researchers and researchers have made new biomimetic designs for wind turbine blades with inspiration from nature. From sea creatures to birds, from the wings of winged insects to tree seeds and plant leaves, the designs of nature have been inspired and many studies have been presented on both new designs and design optimizations (Cognet et. al., 2017).

Some of the most aerodynamically impressive bio-inspired works involve the flight of owls and seagulls. As a result of the researches, it has been determined that the wings of large owl species provide the ability to fly almost silently at frequencies above 1.6 kHz (Oerlemans. et. al., 2009). Studies have shown that owls have this ability with a comb-like leading edge structure, trailing fringes and a soft and porous

upper surface structure. This structure enables efficient use of air in terms of aerodynamics and high transport efficiency at low speeds (Jaworski & Peake, 2013). Teruaki Ikeda et al., inspired by bird wings that enable strong aerodynamic force generation and stable flight, have designed a biomimetic blade for small wind turbines. They used Computational Fluid Dynamics (CFD) to examine the aerodynamic properties of the bird-inspired curved wing morphology they developed and stated that their design had 8.1% better performance than a conventional wing. As a result of the positive results they found, they stated that the biomimetic blade design has an important and great potential for wind turbines and their design can provide an innovative, practical and effective method in wind turbine design for turbulent environments (Ikeda *et. al.*, 2018). Andrew Bodling et al. conducted a numerical research on the design of biomimetic blades to reduce noise in aircraft engines and wind turbines. Inspired by the feather structure of barn owls, the researchers modeled the wing geometry numerically and compared the aerodynamic and aeroacoustic performances with the traditional wing profile. They observed that trailing edge serrations originating from the owl wing structure reduce noise up to 1.8 dB at high frequencies. As a result of their simulations, they stated that the spacing of the serrations is an important design parameter (Bodling *et. al.*, 2017).

Ian A. Clark and colleagues conducted computational and experimental research for a new design inspired by the unique features of the wings of owls that use acoustic stealth during hunting for trailing edge noise control. Inspired by the feather structures on owl wings, the researchers placed the protrusions they developed towards the trailing edge on both the lower surface and the upper surface to prevent boundary layer turbulence. For their design, they tested more than 20 types by making aeroacoustic wind tunnel measurements and, thanks to the useful design they found, they observed a noise reduction of up to 10 dB in trailing edge noise, unlike conventional blades. In addition, they stated that the thickness, density, length and position of the processes to be applied in the design directly affect the effect of the process. The researchers, who obtained positive results in this application in terms of noise, also observed that this application did not have any harmful effects on the handling performance of the wing profile (Clark *et. al.*, 2017). Frank E. Fish and colleagues developed a bio-inspired wind turbine technology inspired by the fins of humpback whales. Using computational fluid dynamics, wing sections with cusps at 100 angles of attack compared to a tubercleless section observed a 4.8% increase in lift, a 10.9% reduction in induced drag, and a 17.6% increase in lift/drag ratio. They also observed that the electricity production of wind turbines with tubercles increased at medium wind speeds. In addition, with this study, the working angle of the wings was increased from 11 degrees to 17 degrees (Fish *et. al.*, 2011).

Weichao shi et al. studied in detail the flow around turbines with and without biomimetic leading edge cusps. With the positive results obtained from the numerical studies, they applied the design to a scaled turbine model with different levels of cusps. It is stated that the hydrodynamic performance of the turbine can increase in the low-end speed ratio region without reducing the maximum power coefficient, which will allow the turbine to start at lower flow rates. The tubercles also help to limit the cavitation zone and thus reduce the noise level. With these advantages, a silent and fast-response turbine

design is created (Shi *et. al.*, 2017). In his thesis, Garrett Wright examined a new design in which he applied the most effective and well-known humpback whale tubercles and owl wing structure of biomimetic design. The aim of the study is to combine the two designs to develop a hybrid design that simultaneously increases efficiency and reduces noise. After his research and testing on hybrid profiles, he found that while the noise reduction aspect of the design was successful, placing the tubercles on the trailing edge caused a decrease in overall efficiency (Wright, 2017).

In a study by H. Johari et al., the effects of leading edge protrusions on airfoil performance were investigated. They observed a decrease in lift and an increase in drag on protruding wings at angles of attack lower than the stopping angle of the basic wing structure. When the stall angle is exceeded, 50% greater lift than the basic wing design was observed. Another issue identified in the studies is that while the protrusions have a significant effect on the performance of the airfoils, the wavelength has little effect (Johari *et. al.*, 2007). On the other hand, plants, tree leaves and tree seeds, which are in constant interaction with the wind and are highly efficient in terms of aerodynamics, have also inspired researchers and many researches have been done in this field. Camilo Herrera and his colleagues designed a wind turbine blade inspired by the seed of a tree called "Triplaris Americana", also known as the ant tree, and presented a wind turbine design with a different design from traditional horizontal axis wind turbines with three blades. Computational fluid dynamics simulation was performed to estimate operational loads. The reason for choosing the selected seed in the study is the rotational movement it makes while falling from the tree. As a result of their experiments with more than 50 different seeds in the vertical wind tunnel they set up for the first stage of the study, they observed an angular velocity of around 1500 rpm and an average free fall velocity of 1.5 m/s. In the second stage, the structure of the wing was characterized from the cross-section of the seed and as a result of the experimental study, they reached a design that started to generate electricity at a wind speed of 2.5 m/s. This special geometry designed has shown that wind turbines have the potential to generate electricity in regions with very low wind speed (Herrera *et. al.*, 2018). Yung-Jeh Chu and Wen-Tong Chong designed a biomimetic wind turbine inspired by the "Dryobalanops Aromatica" seed, also known as Borneo camphor. The designed biomimetic wind turbine provides a better self-starting and a good balance of yaw mechanism at low wind speeds thanks to its high torque (Chu & Chong, 2017). Cory Seidel and colleagues have designed a bio-inspired vertical axis wind turbine from maple seeds and "Triplaris Samara" seeds. They observed that the seeds produced stable leading edge vortices (LEV) that increase the bearing force as they fall to the ground. It has also been shown that leading edge eddies near the root of the wing depend on the geometry of the wing, the Reynolds number, and the angle of attack. As a result, it has been observed that turbine blades inspired by maple seed show the ability to withstand stronger wind speeds (Seidel *et. al.*, 2017).

In their study, Jeppe Johansen and Niels N. Sørensen described the numerical investigation of aerodynamics around a bladed wind turbine blade using Computational Fluid Dynamics (CFD). Five fin models with different twists and curvatures were examined. Of these, four are designated for the pressure side (upstream) and one for the suction side

(downstream). As a result, it has been observed that adding a blade to the conventional wing increases the force distribution over approximately 14% of the wing, resulting in an increase of approximately 0.6% to 1.4% in power generated to wind speeds higher than 6 m/s. Curving the fin downstream further increased power output, but the effect of sweep and pitch angles was not taken into account in obtaining the results (Johansen & Sørensen, 2007).

With the dissolution of the complex structure of nature and the biomimetic designs made, the installation cost, turbine noise and low efficiency problems arising from the design, which hinder the progress of wind turbines as a disadvantage, will come to an end. The new biomimetic designs, which will be designed by improving the work done and inspired by nature, will enable many large and small scale turbines with high efficiency and widespread use, which can meet the installation, operation and recycling costs in a short time, become a part of our lives and export energy demand, even if they are not quiet, low cost. It will end the dependency.

Researchers have tried to reach the ideal wing design by observing nature-inspired wing designs in every area from aquatic creatures to birds, from insects with the ability to fly to plant seeds. Despite their size and weight among sea creatures, humpback whales have inspired researchers thanks to their superior hunting abilities and their unique morphological structures have been transferred to their wing designs. The tubercle protrusions on the fins of humpback whales provide an increase of about 18% in lift/drag force in their wing designs, while also allowing the wings to operate at high angles of attack. When the studies inspired by plant and tree seeds are examined, it is seen that the blade designs inspired by seeds enable the wind turbine blades to start working at low wind speeds such as 2.5 m/s. This provides the potential to generate electricity in regions with low wind speed. In addition, the most impressive biomimetic studies in terms of aerodynamics are those inspired by the wing designs of birds. While there is a significant reduction in the amount of noise and vibration, especially in the wing designs inspired by the owl wing, the use of the notched structure of the owl wing structure on the leading edge, unlike our thesis study, gave positive results in terms of aerodynamics. Nature, which contains many problems and solutions, will ensure that renewable energy sources, especially wind energy, become the energy of the future by removing the obstacles.

2. Biomimetic Wing Design and Aerodynamic Performance Analysis

In this study, the aerodynamic performance parameters of the wind turbine blade structure, which will be inspired by living things in nature, were examined as a fixed blade. Similarly, this study was carried out considering that if the aerodynamic parameter of a fixed blade is better, it will give better results when used in a wind turbine. The winglet, which significantly affects the fuel consumption and aerodynamic performance of aircraft, has also been a source of inspiration for us in this study. In addition, the wing tip vortex reducing endless wing, which is similar to the working logic of the winglet, is investigated in wind turbine blade design in this study. See in this (Uzun & Çoban, 2021). in the numerical analysis of the curved wing and winglet structure, it was observed that the aerodynamic performance improved with the change of the curvature percentage. In this study, the

aerodynamic performance values were investigated numerically by adding the endless wing and the up and down curved shape of the wing in accordance with the wing structure. In this study was carried out at different speeds at a constant angle of attack, and flow images and aerodynamic parameters were given graphically.

2.1. Design parameters

Because of its overpowering in the wind turbine industry, it is very sensitive to changes in airfoil and design. In wind turbine blade design, turbine blade aerodynamics and wind load are important parameters. This section will shortly describe the main parameters that affect the performance of modern wind turbine blades. While designing the wing, drag and lift force, Betz limit, losses and wing element theory criteria should be considered.

In today's modern wind turbines, special airfoils are used to obtain ideal power from the blade. It is aimed to improve the carrying force in the airfoil structure. In these special profiles, two different curved blade structures are formed above and below a beam line. The fact that the upper curve has a more humped structure creates a pressure difference between the two surfaces and the tendency of the air in the high pressure area to move to the low pressure area creates the bearing force.

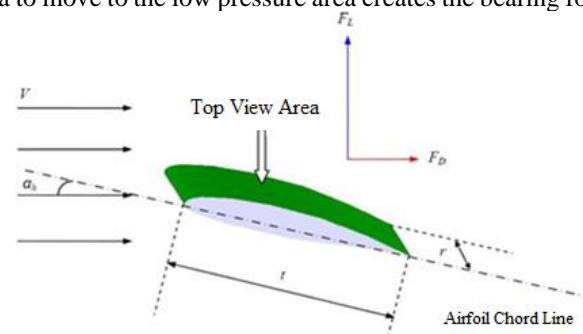


Figure 1. Forces acting on the airfoil

$$F_D = 1/2 C_D \rho AV^2 \quad (2.1)$$

$$F_L = 1/2 C_L \rho AV^2 \quad (2.2)$$

Here, C_L is the lift coefficient, and C_D is the drag coefficient. C_L , C_D , C_L/C_D (ϵ) values are determined experimentally at certain Reynolds number and different angles of attack, and these values indicate the quality of the airfoil.

The dimensions of the wind turbine are considered to be directly related to the aerodynamic structure in order to obtain the best energy from the wind. No matter how good the installed turbine is, there is an upper limit to the energy that the system can obtain from the wind. According to the Betz limit, the energy that can be obtained from the wind in the ideal environment is theoretically $2/3$ of the wind.

2.1.1. Tip speed ratio

The tip speed ratio is expressed as the relationship between the free flow speed and the wind turbine blade, and it has an important place in optimizing other parameters. (Schubel *et al.*, 2012):

$$\begin{aligned} \lambda &= \text{Tip Speed Ratio} \\ \Omega &= \text{Rotational Speed (rad/s)} \\ r &= \text{Radius} \end{aligned} \quad (2.3)$$

$$\lambda = \frac{\Omega r}{V_w} \quad V_w = \text{Wind Velocity}$$

Optimizing wing tip speed depends on noise, torque force, aerodynamics and vibrations. Efficiency will tend to decrease with increasing noise, if the wing tip speed, which is taken into account together with other variables, increases, the efficiency of wind energy will increase (Gasch *et. al.*, 2002).

2.1.2. Wing plan shape and quantity

The ideal plan form of a HAWT rotor blade is defined using the BEM method by calculating the beam length according to the Betz limit, local air speeds, and blade lift. The simplest theory Based on the Betz optimization , several theories exist to calculate the optimum beam length varying in the complexity (Hau , 2006).range. For wings with six to nine tip velocity ratios using aerofoil sections with negligible drag and tip losses, Betz's momentum theory gives a good approximation [46]. In the case of low tip speeds, high friction aerofoil sections, and wing sections around the hub, this method can be considered inaccurate. In such cases, tracking and drag losses should be taken into account (Dominy *et. al.*, 2002). The Betz method gives the basic shape of the modern wind turbine blade (Figure 2). But in practice, more advanced optimization methods are often used.

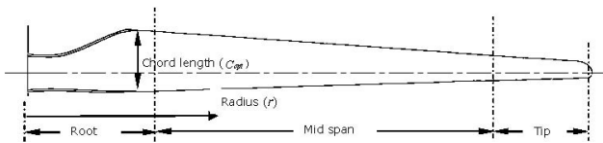


Figure 2. A typical wing plan and zone classification (Schubel *et. al.*, 2012)

Table 1. Optimum beam length

	r, radius (m)
	n, number of wing blades
	C_L , lift coefficient
	λ , local tip speed ratio
	V_r , local airspeed
	U, wind speed (m/s)
	U_{wd} , Designed wind speed
	C_{opt} , Optimum chord length
$C_{opt} = \frac{2\pi r}{n} \frac{8}{9C_L} \frac{U_{wd}}{\lambda V_r}$	
$V_r = \sqrt{V_r^2 + U^2}$	

Assuming that a reasonable lift coefficient is maintained, using a wing optimization method produces wing plans mainly dependent on the design tip speed ratio and the number of wings (Figure 3). Low tip speed ratios produce a rotor with a high stiffness ratio, which is the ratio of blade area to the area of the swept rotor. It is beneficial to reduce the strength area, as it leads to a reduction in material usage and thus production costs. However, problems are associated with high end speeds (Schubel *et. al.*, 2012).

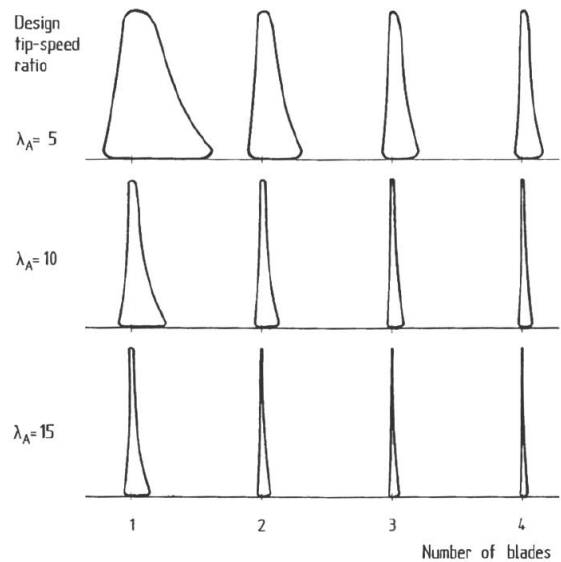


Figure 3. Optimum blade shape tip speed ratios and blade number for alternative design (Schubel *et. al.*, 2012)

2.2. Boundary conditions

The calculation area has been extended by 15 lengths (C) above and below the nose of the airfoil. Intercalarily, 20C was applied from the pressure outlet surface. The velocity input boundary condition was applied in the up and down directions at a speed of 13 m/s. Non-slip boundary condition is used on solid surfaces. Figure 4 shows all these setups for simulations.

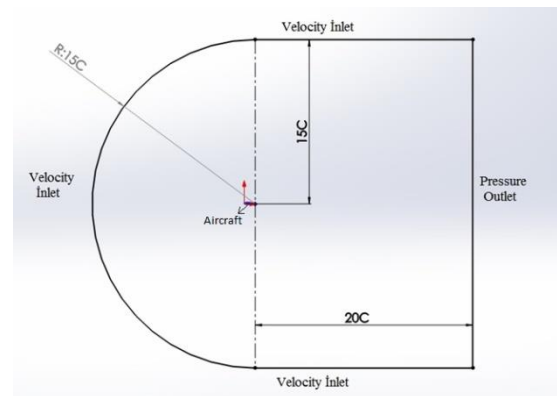


Figure 4. The dimensions and boundary conditions of the computational domain

Velocity components are defined for each angle of attack. The x component of velocity is calculated by $x=13 \cdot \cos \alpha$ and the y component of velocity is defined by the formula $y=13 \cdot \sin \alpha$ where α is the plane's angle of attack in degrees.

2.3. Grid Independency study

The grid used for the simulations is created with the CFD Mesh program and the mesh and all nose options are shown in Figure 5, the Patch Conforming / Sweeping method used. In order to eliminate mesh effects, the optimum number of mesh elements should be determined. Increasing the number of elements provides more accurate results, while using more elements increases the solving time. For this reason, network independence study was carried out with 100k, 200k, 400k, 800k, 1500k and 5000k elements. In Figure 5, the variation of the lift coefficient with different element numbers at 0 degree angle of attack is given. The lift coefficient value does not change much after 800k element count. In other words, it can be said that 2400k elements are sufficient for correct results.

In addition, the convergence criteria were chosen as 10⁻⁶. Approximately all analyzes were completed between 500-1000 iterations. Used computer with Intel(R) Xeon(R) CPU E5-1620-0 @ 3.60 GHz x64 bit and 8GB ram. The maximum analysis time for a simulation is 4 hours.

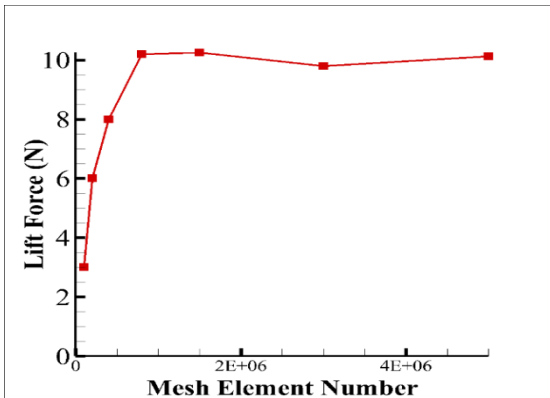


Figure 5. Variance of lift coefficient and number of elements

Table 2 gives the mesh properties of the our biomimetic wing design. Patch Conforming / Sweeping is selected as the mesh method and the smallest mesh element size is 1mm.

Table 2. Mesh properties

MESH PROPERTIES	
Minimum Element Size	0.0053056 m
Number of Elements	819427
Maximum Size	0.61847 m
Orthogonal Quality	0.19604
Skewness	0.80212
Growth Rate	1.115
Curvature Normal Angle	18°
Mesh Method	Patch Conforming / Sweeping

Figure 6 shows the dynamic pressure, velocity magnitude and pattline velocity analysis results of the fixed wing, respectively. The orthogonal quality gives an idea about mesh quality in wind blade and airfoil analysis. The range of 0.95-1.00 is excellent, 0.70-0.95 is very good, 0.20-0.69 is good, 0.10-0.20 is receivable, 0.001-0.10 is poor and finally 0- 0.001 is considered as inadmissible (Görgülü *et. al.*, 2021)

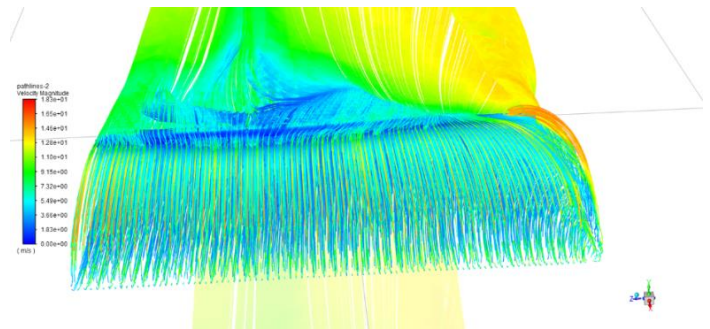
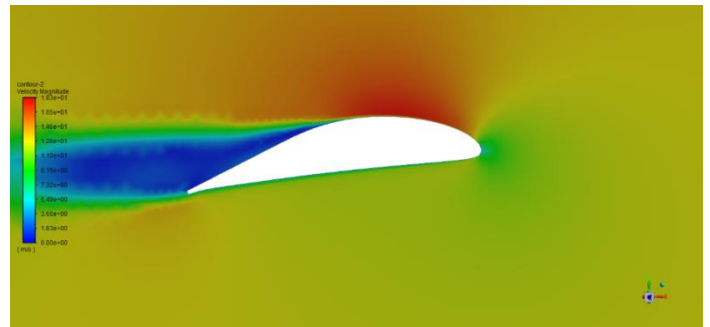
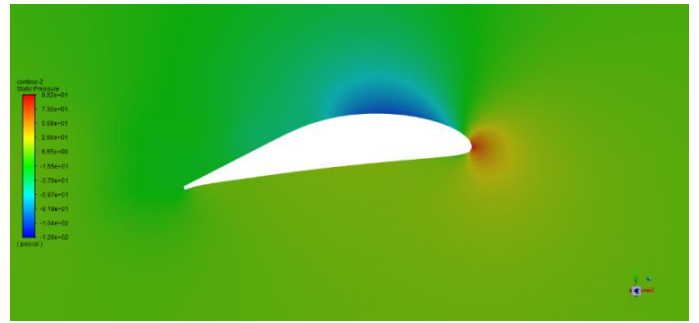
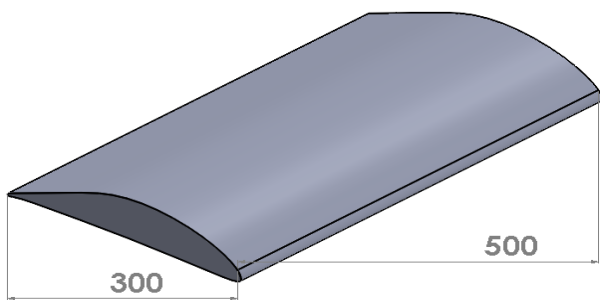
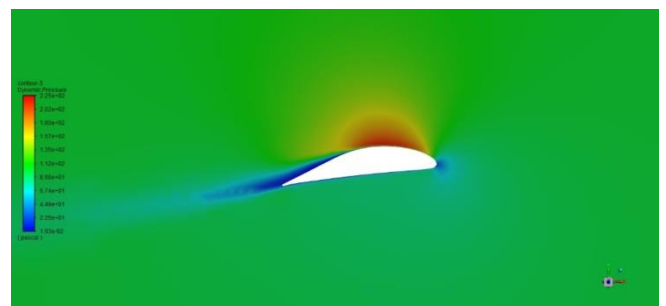


Figure 6. Fixed wing dynamic pressure, velocity magnitude and pattline velocity analysis

In figure 7, respectively, dynamic pressure, velocity magnitude and pattline velocity analysis results of the endless wing1 is given.



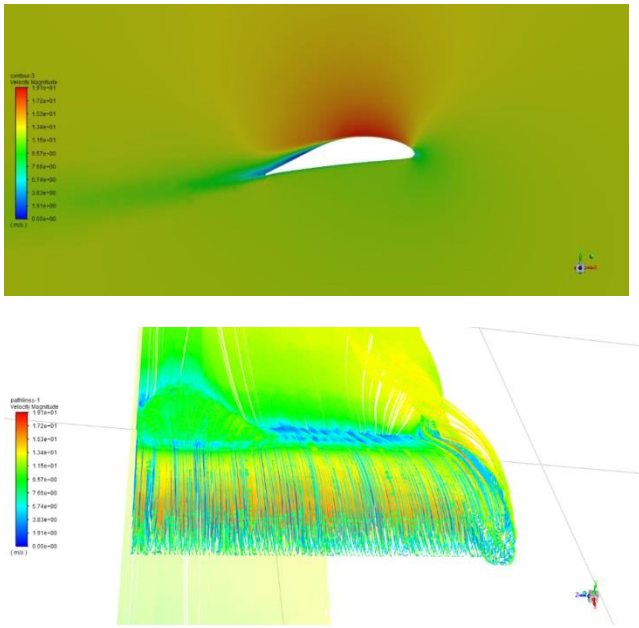


Figure 7. Endless wing1 dynamic pressure, velocity magnitude and pattline velocity analysis

Figure 8 shows the dynamic pressure, velocity magnitude and pattline velocity analysis results of the endless wing2, respectively.

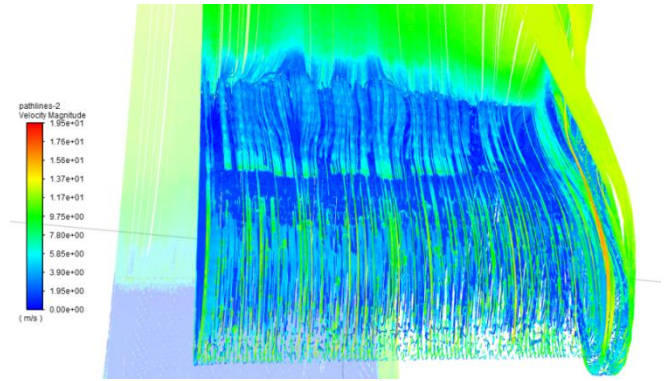


Figure 8. Endless wing 2 dynamic pressure, velocity magnitude and pattline velocity analysis

In figure 9, respectively, dynamic pressure, velocity magnitude and pattline velocity analysis results of the endless wing 3 is given.

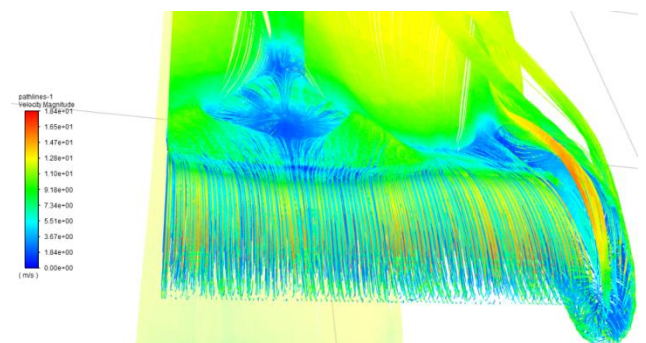
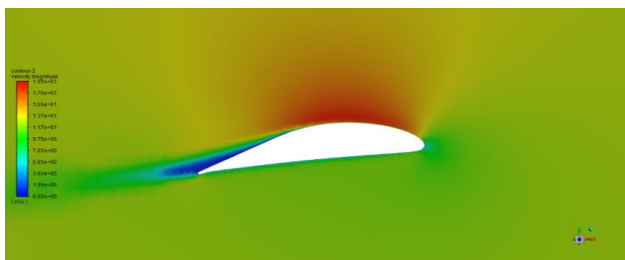
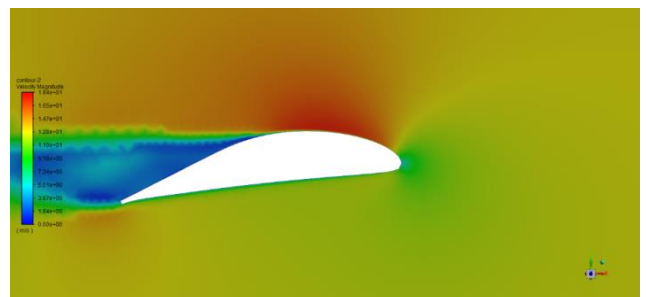
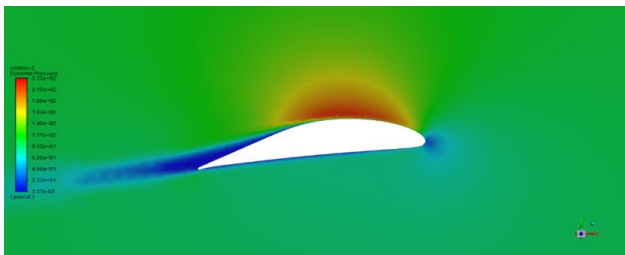
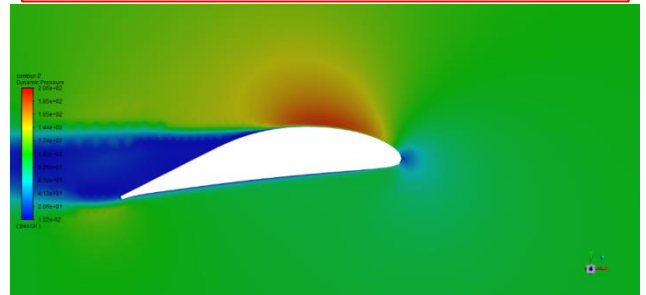
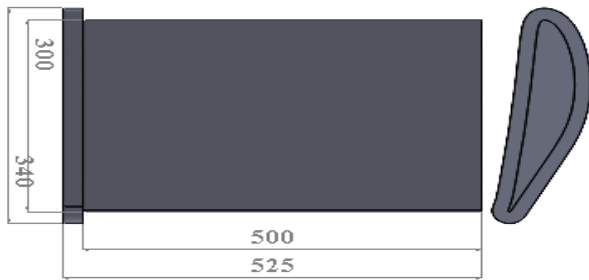


Figure 9. Endless wing 3 dynamic pressure, velocity magnitude and pattline velocity analysis

Figure 10 shows the dynamic pressure, velocity magnitude and pattline velocity analysis results of the curved down wing, respectively.

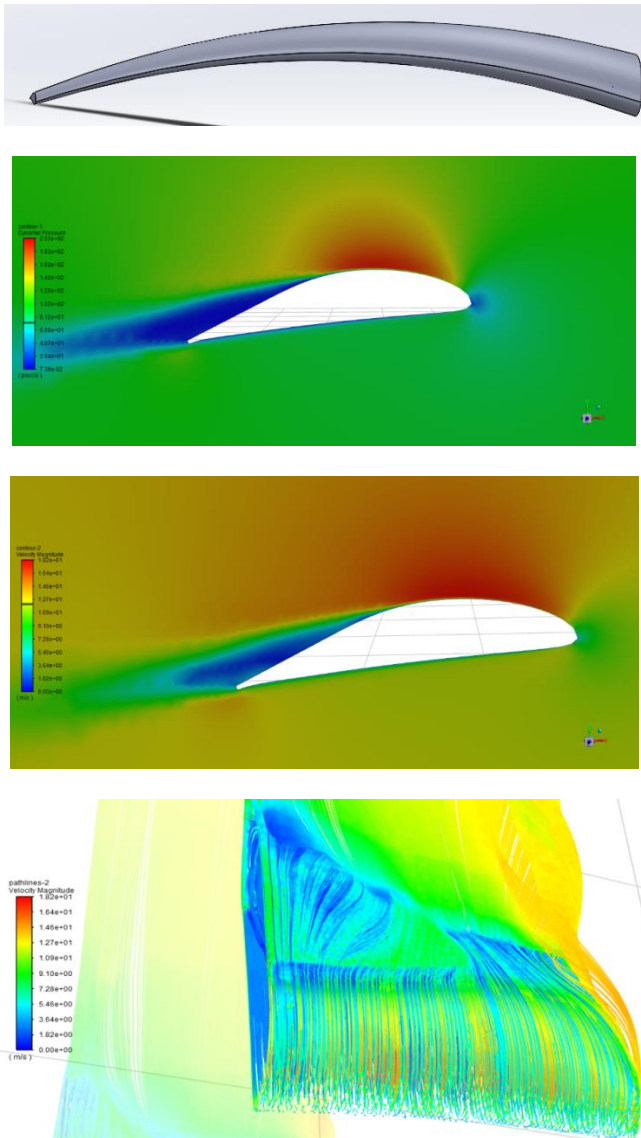


Figure 10. Curved down wing dynamic pressure, velocity magnitude and pattline velocity analysis

In figure 11, respectively, dynamic pressure, velocity magnitude and pattline velocity analysis results of the curved up is given.

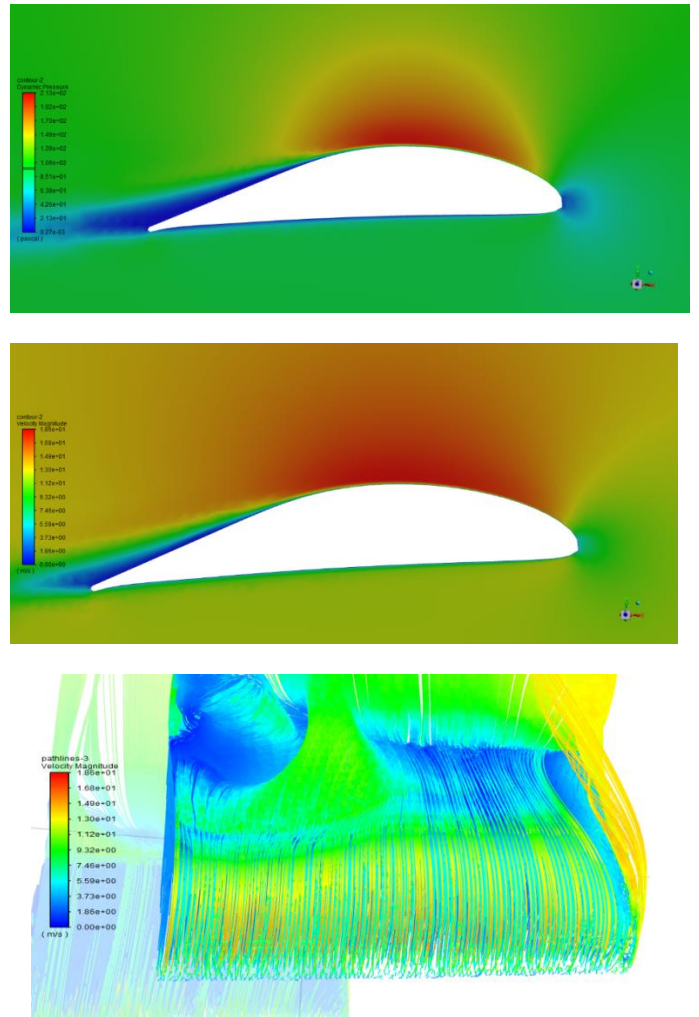
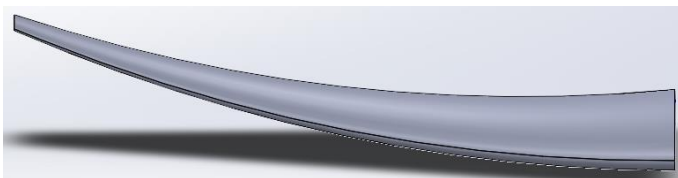


Figure 11. Curved up wing dynamic pressure, velocity magnitude and pattline velocity analysis
Detailed specifications of the designed wing profiles are given in Table 3.

Table 2. Detailed specifications of the designed wing profiles

	Angle of the wing tip	Radius(mm)
Winglet 1	70°	5
Winglet 2	45°	5
Winglet 3	30°	5
	Notch width(mm)	Quantity(pcs)
Notched Leading Edge 1	2,5	4
Notched Leading Edge 2	2,5	6
Notched Leading Edge 3	2,5	14
	Endless wing length(mm)	Wing tip chord length(mm)
Curved Wing+	12	8
Endless Wing 1		
Curved Wing+	18	8
Endless Wing 2		
Curved Wing+	27	8
Endless Wing 3		
Curved Wing+	35	8
Endless Wing 4		

In Figure 12, the lift force values of the fixed wing and the curved wing are compared.

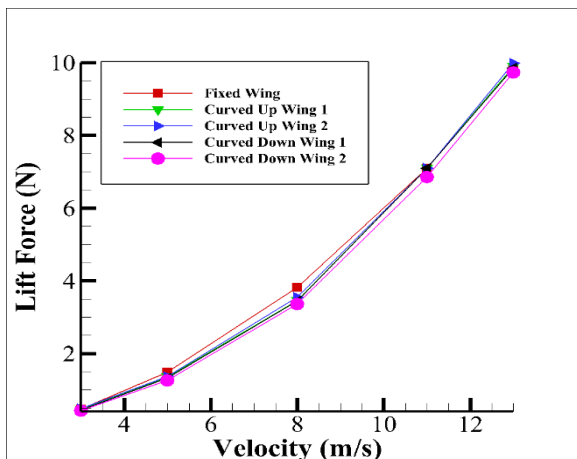


Figure 12. Lift force values fixed wing and curved wing

In Figure 13, the lift/drag force values of the fixed wing and the curved wing are compared.

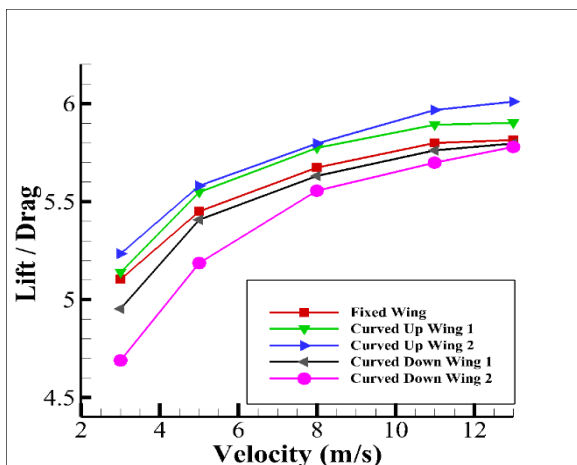


Figure 13. Lift/drag force values fixed wing and curved wing
In Figure 14, the drag force values of the fixed wing and the endless wings are compared.

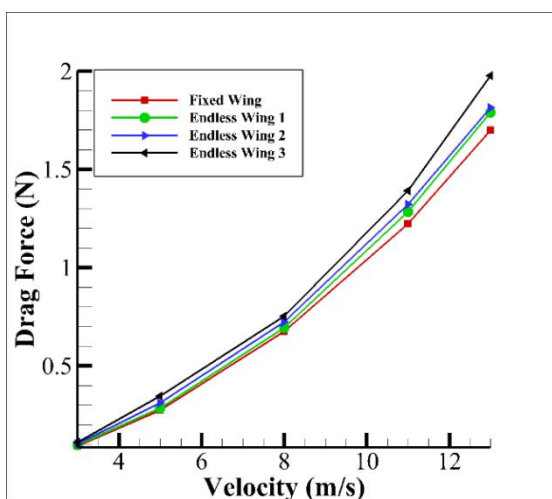


Figure 14. Drag force values fixed wing and endless wings.

In Figure 15, the lift values of the fixed wing and the endless wings are compared.

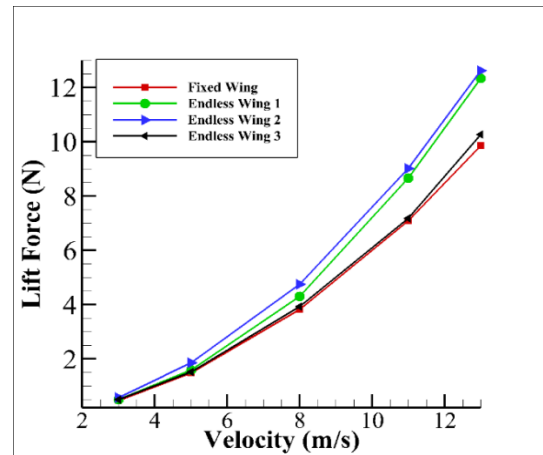


Figure 15. Lift force values fixed wing and endless wings.

In Figure 16, the lift/drag force values of the fixed wing and the endless wings are compared.

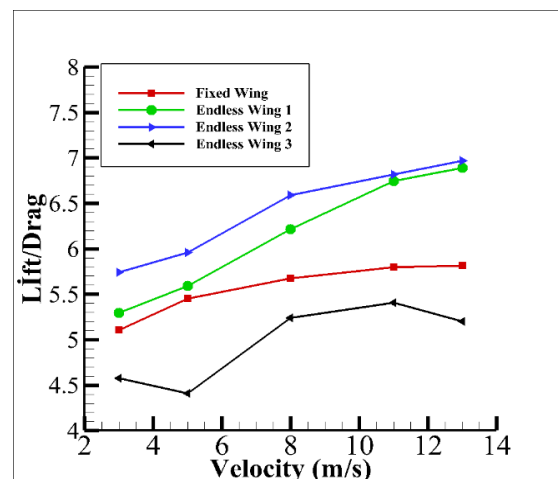


Figure 16. Lift/drag force values fixed wing and endless wings.

In this study, the flow analysis and aerodynamic parameters of fixed wing and variable sized fins mounted on the wing tip were compared. The endless wing structure was preferred from the same structure as the wing profile, but the variation in which size the infinite wing would give better results was examined by applying it. When the flow images are examined, while the flow disrupts the upper surface of the wing by forming a vortex due to the pressure difference from the tip of the fixed wing, this distortion is partially prevented when the endless wing structure is applied. However, when the size of the endless wing structure is increased, for example, for the endless wing 3, the increase in drag force has begun to affect the aerodynamic performance negatively. When the endless wing 1 and 2 structure is compared with the fixed wing, it is clear that the aerodynamic performance values improve when the graphs are examined, since the wing tip vortices tend to decrease compared to the fixed wing. When the dynamic pressure images of the fixed wing and the endless wing are examined, it is clear that the pressure value naturally improves in terms of flow retention, as the upper part of the wing partially gets rid of the vortex. In Figure 16, the ratio of lift force to drag force, which is the aerodynamic performance values of fixed wing and endless wing operation, is given.

Here, it has been seen that the aerodynamic performance value of the fixed wing increases when the endless wing is added to the wing tip, and the design we call infinite wing 2 has the highest aerodynamic performance, and when the endless wing 3 dimension is changed, the performance value decreases due to the increase in drag force.

Similarly, inspired by the wing structure of the owl bird, the change of aerodynamic performance values was examined by giving an curved up and down from the middle part of the fixed wing. In figures 14 and 15, the solid design, aerodynamic parameters and flow analyzes of the curved up and down are given in detail. The flow separation bubble on the wing when the slope is given downwards in the wing structure and as a result, the losses in aerodynamic performance are clearly seen. When figure 16 is examined, it is seen that the lift divided by drag force values improve when the curve is upwards compared to the fixed wing, while the performance values decrease when the curve is downwards.

3. Wind Tunnel Analysis

It is used to test the aerodynamic properties of real or reduced-size parts and vehicles placed in the air tunnel (or wind tunnel) under controllable conditions. Different mechanisms are used according to the required speeds, as well as providing a smooth gas (or air) flow. Investigation of wind vortices formed around high-rise buildings, from air tunnels that used to be used only to control the aerodynamic forms of airframes, today both for the determination of the shape of projectiles and road-rail vehicles, as well as for the safe discharge of wind loads and gases of high-rise structures, bridges, power transmission lines and radar scanners. For this purpose, the experiments carried out to investigate how the snow falling in the regions where the highways are located can be counted. Experimental study of our wind turbine designs was carried out in the DNS brand T-490 model wind tunnel experiment set in the mechanical engineering inventory of Iskenderun Technical University.



Figure 17. T-490 wind tunnel

The T-490 air tunnel is designed to conduct experiments in the fields of aerodynamics and fluid mechanics. This air tunnel is an open air tunnel. In this type of air tunnels, air is taken from the atmosphere and given back to the atmosphere. The nozzle part controls the stable distribution of velocity in the closed measuring section.

3.1. Technical detail

Air velocity measurement, fan speed control, For airflow and aerodynamic experiments, large-scale intermediate channels, open type air tunnel, flow regulator, Transparent measuring section, Tunnel type axial fan, Drag and lift force with different apparatus, measurement, Blade model pressure distribution, Cylindrical pressure distribution.

3.2. Device dimensions

Device dimensions are A x B x H: 2500 x 670 x 1250 mm.

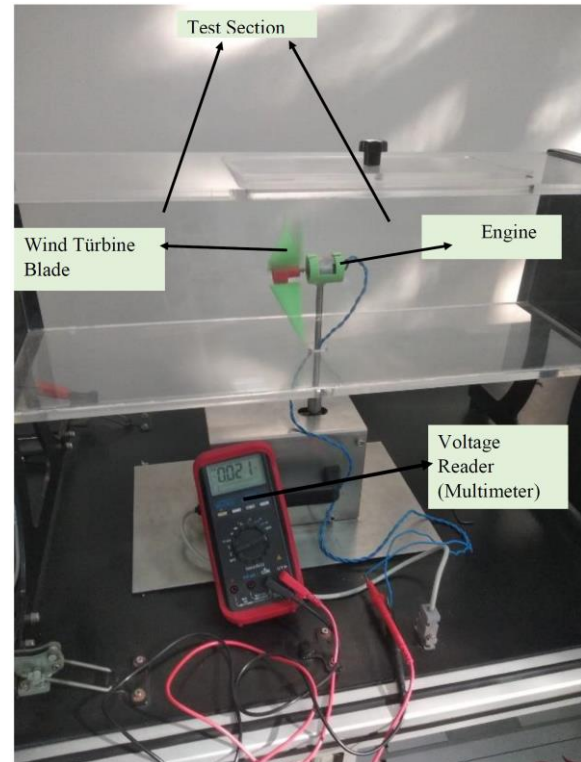


Figure 18. Wind turbine test system

In the previous sections, we talked a lot about the numerical analysis results and aerodynamic performance criteria of our wind turbine blade designs as fixed blades. In this section, it has been tried to determine the voltage values produced by the variables inspired by nature at different speeds and different connection angles with the help of an electric motor in the wind tunnel of the wind turbine blade designs experimentally. Here, the wind turbine hub, which is placed in the wind tunnel test flow region, the blade designs are mounted on the engine hub, and the cable connections of the engine are directly connected to the multimeter. When the wind tunnel is activated at different speeds, the flow rate information is obtained from the flow rate sensor in the diffuser area of our tunnel, and the multimeter gives us the generated power as voltage. The voltage values obtained were obtained by taking the test average of at least 3 minutes for each experiment. The aim of this study is to obtain a design that can produce higher power than different wind turbine blade designs.

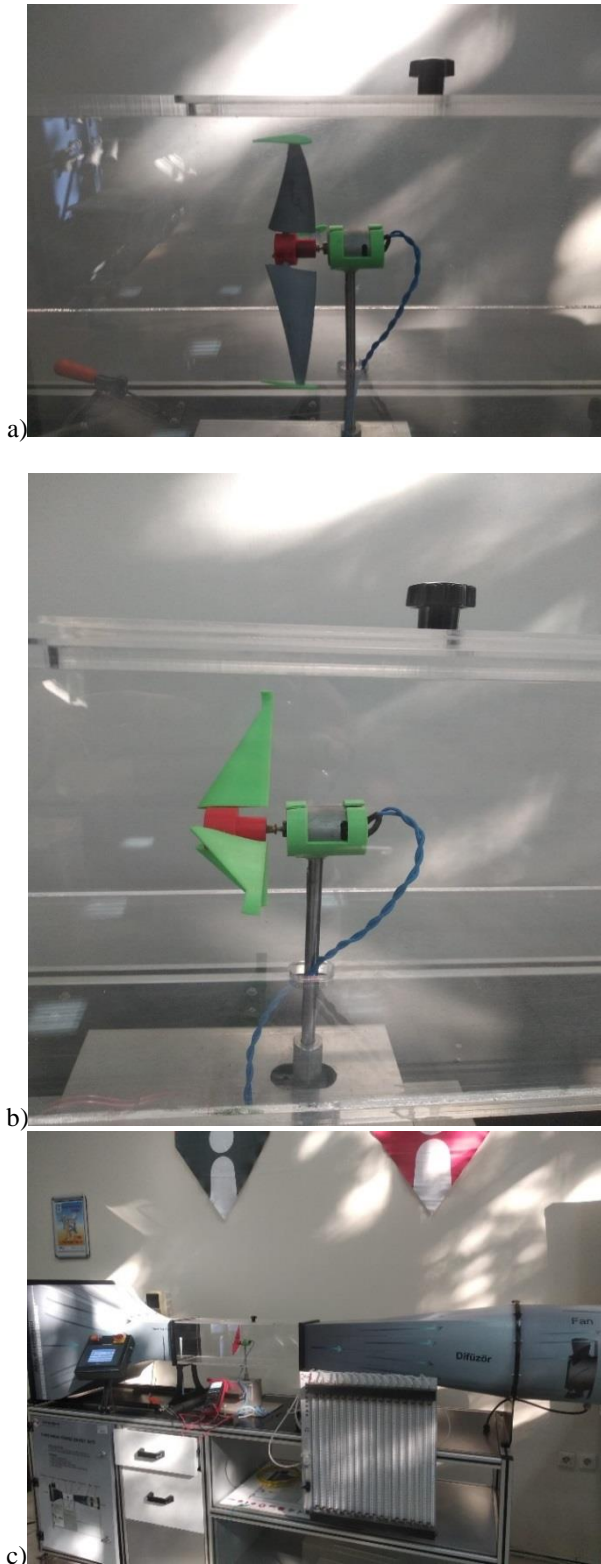


Figure 19. View of wind tunnel from different angle

Therefore, the voltage value produced will give important information about learning which turbine blade design is more advantageous.

3.3. Endless blade effect in wind turbine design

In this section, inspired by the owl wing structure, the fixed wing structure is designed as curved wing and the power produced experimentally is measured when the endless wing structure is mounted on the wing tip. In figure 20, the dimensions of the endless wings placed on the curved wing tip

are applied as variable and their size information is shown. Here, the meaning of the designs named endless wing1 or endless wing 2 and how they differ from the wing tip chord length are clearly given.

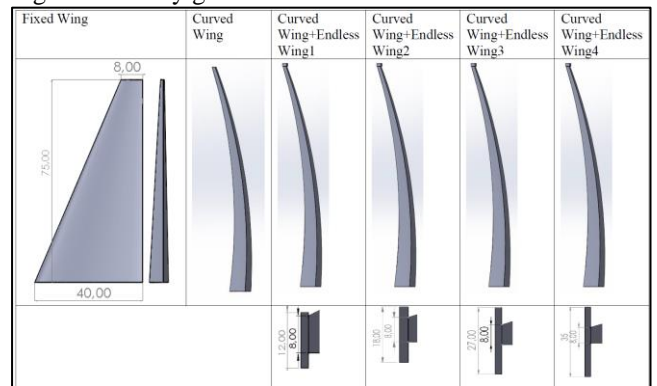
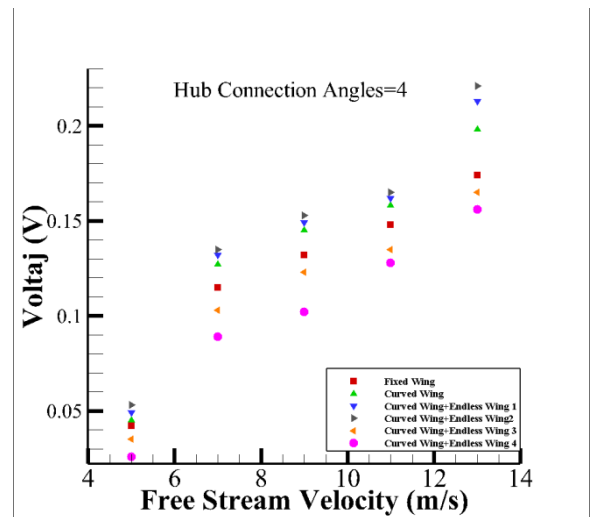
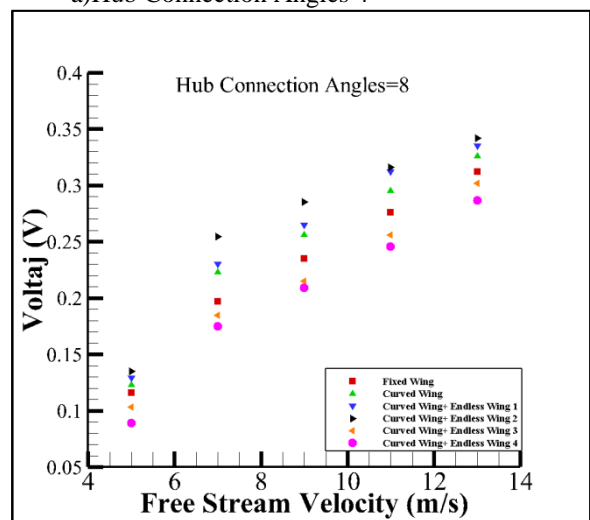


Figure 20. Endless blade designs

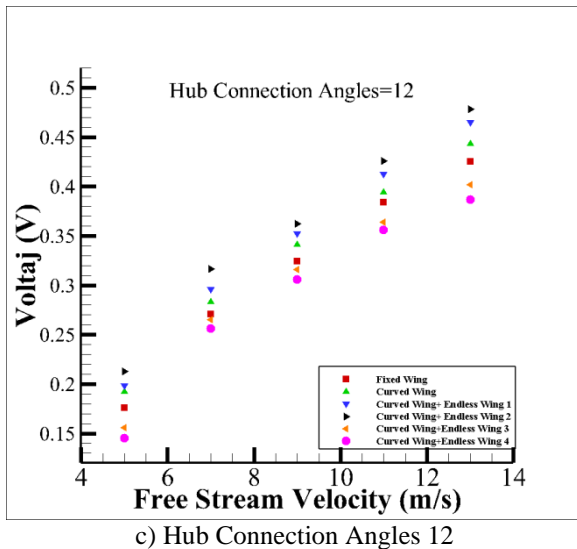
In the design named as Endless wing 1, while the wing tip is 8 mm, the mounted endless wing chord length is designed as 12 mm, and for the endless wing 4 it is designed as 35 mm. Here, the endless wing structure is obtained from the wing profile and enlarged at the same rate from all parts.



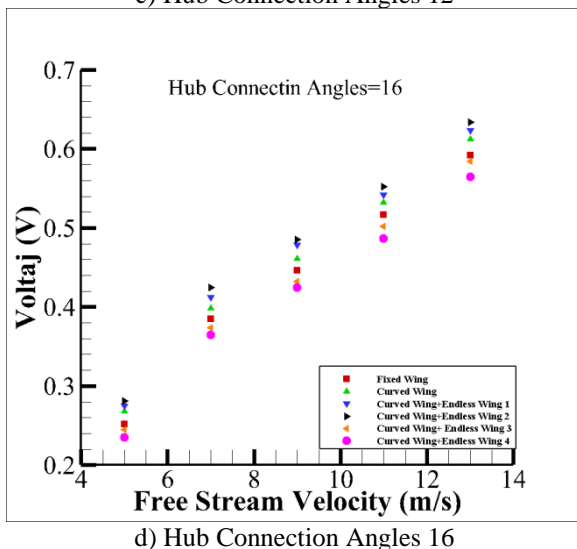
a) Hub Connection Angles 4



b) Hub Connection Angles 8



c) Hub Connection Angles 12



d) Hub Connection Angles 16

Figure 21. Voltage values of endless blade designs at different speeds

In figure 21, the voltage values obtained from the endless blade structures designed at different connection angles and different wind speeds are given. In figure 22, a visual about how the wind turbine blades are connected to the hub and how this hub is mounted with the engine is given.

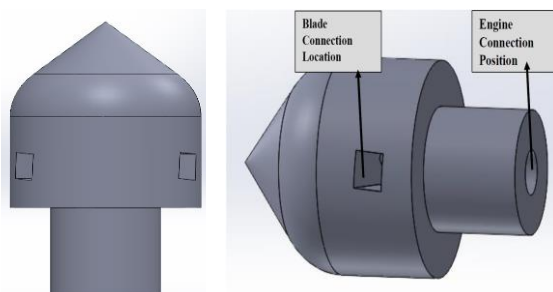


Figure 22. Blade hub connection

The measurements taken here were carried out at different hub connection angles, so different hubs were produced with different hub connection angles. Changing the hub connection angle corresponds to the angle of attack in the fixed wing system, but in systems such as power generation with the propeller, it creates a similar operation to the pitch angle. In Figure 21, 4 different graphs are given in these graphs. In these graphs, the information about how the endless wing structure

that we add to the wing tip will be beneficial as a wind turbine according to different flow velocity values at different hub connection angles is presented. When the graphs given comparing the fixed wing and the endless wing are examined, the voltage value increased when the endless wing is placed on the wing tip, but the voltage value started to decrease because the increase in the endless wing chord length after a certain value produces extra drag force. hub connection angles were applied between 4-16 degrees, and when working with connection angles higher than 16 degrees, voltage generation decreased due to airfoil stall. In section 2, the results of constant flow analysis and flow visuals of designs with endless blades are also given, and it has been observed that the blade tip vortexes decrease when endless blades are applied. Based on this, it was thought that the endless blade application would be beneficial in wind turbine blade design. When the results were examined, it was seen that the voltage values produced were improved when the endless blade application was made in the right dimensions.

3.4. Winglet blade effect in wind turbine design

In this section, a wind turbine blade design has been made by adding a winglet to the fixed blade tip, and the voltage value produced by the designs defined as winglet 1, winglet 2 and winglet 3 has been measured. In the design called winglet 1, the fixed wing length and width were kept constant, and the design was obtained with the same airfoil structure as the wing profile, making an angle of 70 degrees with the vertical to the wing tip.

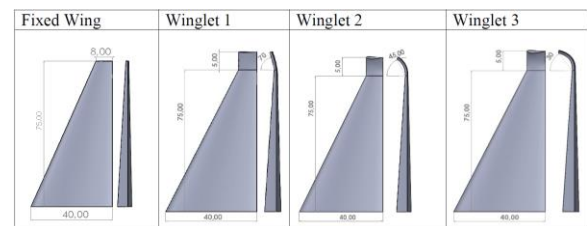
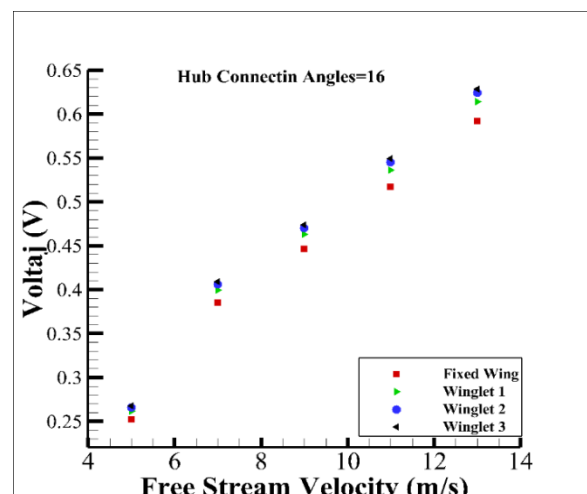


Figure 23. Designs with winglet mounted on the wind turbine blade tip

In the designs called winglet 2 and winglet 3, the fixed wing and the length and width are the same, and the angles they make with the vertical are 45 and 30 degrees, respectively. It is clear that aerodynamic performance values improve when a winglet is mounted on the wing tip of an unmanned aerial vehicle [20]. For this reason, it is significant that adding a winglet to the end of the wind turbine blade will also contribute to the electrical energy produced.



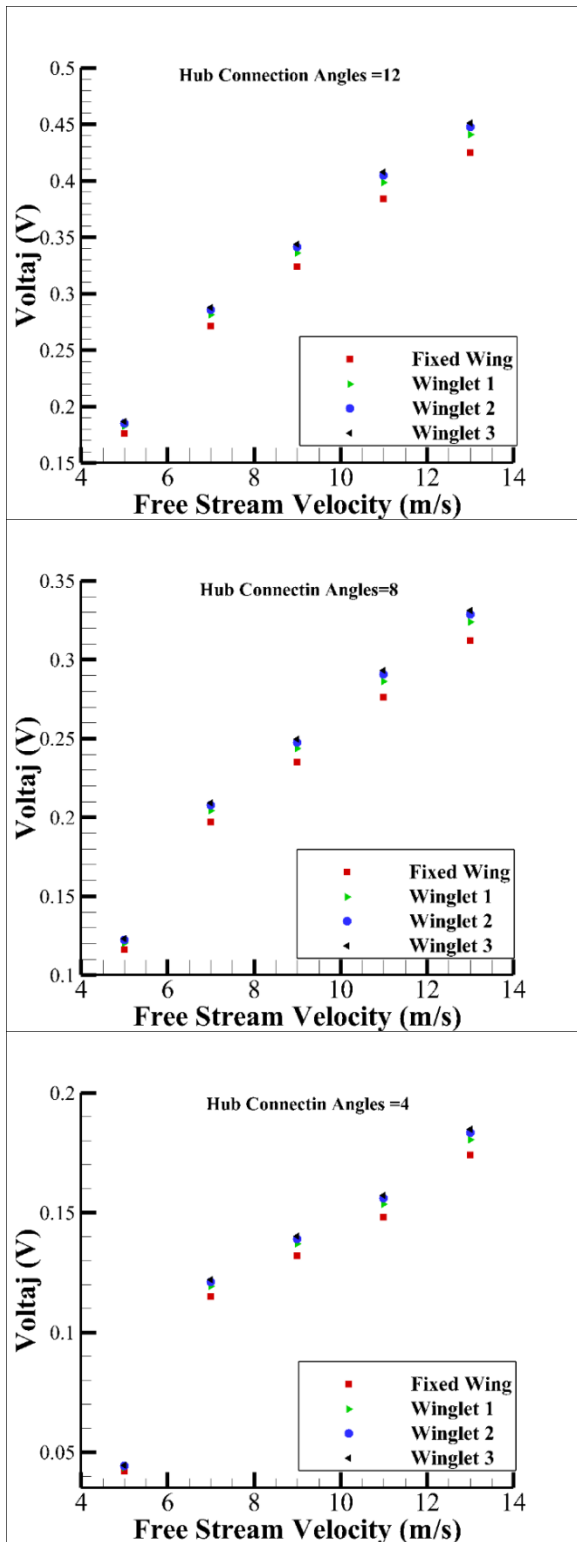


Figure 24. Voltage values of winglet blade designs at different speeds

In figure 24, the comparison of the voltage values obtained at different flow rates of the designs named winglet 1, winglet 2 and winglet 3 at different hub angles with the fixed blade is given. The winglet wing structure placed on the tip of the wing structure improves the flight performance of the aircraft, as it helps to reduce the tip vortices. Similarly, when the winglet usage in the wind turbine blade structure is examined, the generated voltage value has increased. The use of winglets increases the number of revolutions in the same environment as the wind turbine produces less drag force in the blade

structure compared to the fixed blade. Free stream flow velocity values were preferred between 3-13 m/s. Since wind energy generally causes a decrease in efficiency above 13 m/s, and 3 m/s is the most inefficient of our designs to start power generation.

3.5. Notched leading edge blade effect in wind turbine design

When the trailing edges of the owl's wing structure or the wing structure of other similar birds were examined, it was observed that there were gaps between their feathers. There are designs in different technological fields inspired by nature. Especially in the aircraft engine exhaust part, it is clear that the logic of this actually reduces the noise level in the hunting mechanism, so it can be preferred in areas where noise and vibration reduction is desired. In this study, the study was carried out with the thought that it would be useful to produce the wind turbine blade design inspired by this.

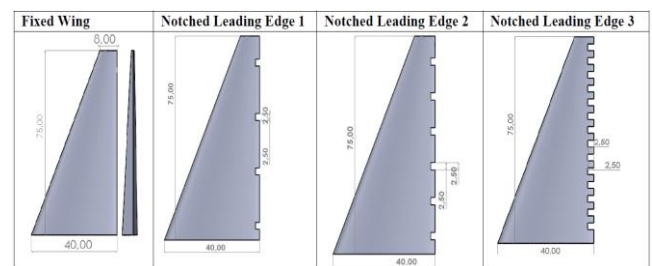
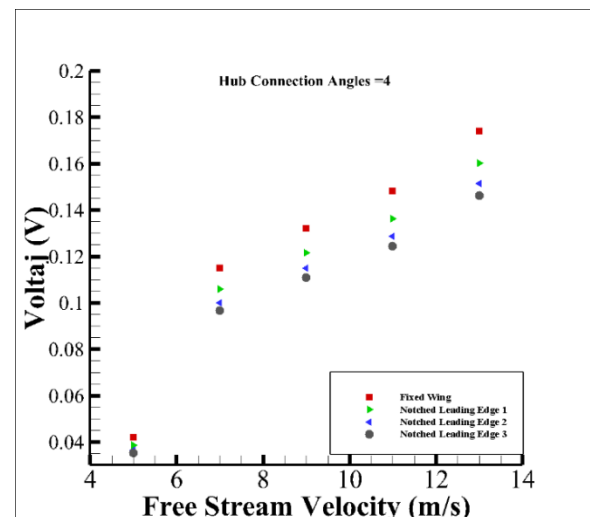


Figure 25. Designs with Notched Leading Edge mounted on the wind turbine blade tip

In figure 25, it is clearly shown in what size and how often the notched leading edge wing structure is added to the trailing edge with different designs in the fixed wing design.



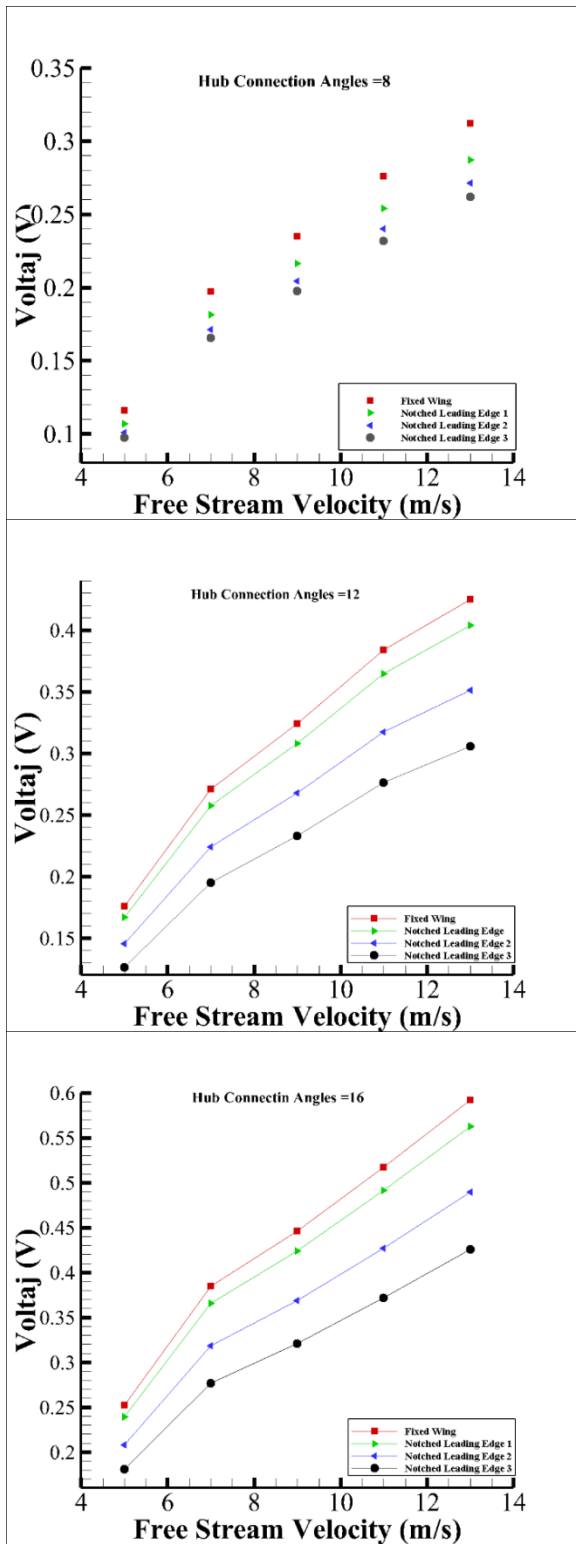


Figure 26. Voltage Values of Notched Leading Edge Blade Designs At Different Speeds

In figure 26, the comparison of the voltage values obtained at different flow rates of the designs named Notched Leading edge 1, Notched Leading edge 2 and Notched Leading edge 3 at different hub angles with the fixed blade is given. When the velocity and voltage changes of the notched leading edge wing designs compared with the fixed wing are examined, the presence of leading edge wing on the trailing edge or the increase in its frequency increase the cause the flow separation and turbulence to increase. Therefore, as a result of the notched leading edge blade application, the efficiency decreases and

the voltage value produced decreases. However, it should be examined whether there is any improvement in vibration or noise and if there is an increase in efficiency in wind energy as a result of this effect.

4. Conclusion

In this study, it has been tried to maximize the efficiency of wind energy with a new design inspired by nature in the blade design of the wind turbine. First of all, the curved wing shape in the wing structure of the owl bird during flight attracted our attention. In the previous study, it was seen that the curved blade structure was beneficial in the efficiency of the wind turbine compared to the fixed blade, and together with these, the endless blade was integrated into the tip of the curved blade structure and tested in the wind tunnel. Variations in the voltage value produced depending on the size of the endless wing structure added at the wing tip were observed. An improvement of up to 15% was observed in the designs we named as curved wing1 and curved wing 2. Similarly, in the designs we named curved wing 3 and curved wing 4, when the endless wing size was enlarged, the opposite effect was observed, that is, a voltage drop of up to 12% was observed as the drag force increased too much. In section 3.4, the comparison of the fixed wing and the fixed wing structure with the winglet structure placed at the tip is given, and it is explained how the use of the winglet and the change of the winglet angle affect the voltage generation. An improvement of about 6% in the voltage values produced by the use of winglet in the fixed wing structure was obtained at different speeds and different hub angles. In section 3.5, a comparison of the voltage value produced by the notched leading edge and the use of fixed blade design as a wind turbine is given. When notched leading edge is applied to the trailing edge of the wing structure, it causes the flow to be disrupted and the vortices to increase at the trailing edge. There is definitely a reason why there is this feature in living things in nature, but there is no benefit in terms of voltage or energy production when it is used in wind turbine blade structure. When the generated voltage values are examined, it is observed that the energy value produced has decreased by 30% with the increase in the number of notched leading edges.

Ethical approval

Not applicable.

Acknowledgement

The authors would like to thank the Erciyes University Research Fund for their financial support of present work (FYL-2020- 10291).

References

- Bodling, A., Agrawal, B. R., Sharma, A., Clark, I., Alexander, W. N., & Devenport, W. J. (2017). Numerical investigations of bio-inspired blade designs to reduce broadband noise in aircraft engines and wind turbines. In 55th AIAA Aerospace Sciences Meeting (p. 0458).
- Chu, Y. J., & Chong, W. T. (2017). A biomimetic wind turbine inspired by *Dryobalanops aromatica* seed: Numerical prediction of rigid rotor blade performance with OpenFOAM®. *Computers & Fluids*, 159, 295-315.

- Clark, I. A., Alexander, W. N., Devenport, W., Glegg, S., Jaworski, J. W., Daly, C., & Peake, N. (2017). Bioinspired trailing-edge noise control. *AIAA Journal*, 55(3), 740-754.
- Cognet, V., Courrech du Pont, S., Dobrev, I., Massouh, F., & Thiria, B. (2017). Bioinspired turbine blades offer new perspectives for wind energy. *Proceedings of the Royal Society A: Mathematical, Physical and Engineering Sciences*, 473(2198), 20160726.
- Dominy, R.; Lunt, P.; Bickerdyke, A.; Dominy, J. Self-starting capability of a darrieus turbine. *Proc. Inst. Mech. Eng. Part A J. Power Energy* 2007, 221, 111–120.
- Fish, F. E., Weber, P. W., Murray, M. M., & Howle, L. E. (2011). The tubercles on humpback whales' flippers: application of bio-inspired technology.
- Gasch, R.; Twele, J. *Wind Power Plants; Solarpraxis: Berlin, Germany*, 2002.
- Görgülü, Y. F., Özgür, M. A., & Köse, R. (2021). CFD analysis of a NACA 0009 aerofoil at a low Reynolds number. *Politeknik Dergisi*, 1-1.
- Hau, E. *Wind Turbines, Fundamentals, Technologies, Application, Economics*, 2nd ed.; Springer:Berlin, Germany, 2006.
- Herreraa, C., Correea, M., Villadaa, V., Vanegasb, J. D., Garciaa, J. G., Nieto-Londonoa, C., & Sierra-Pérez, J. (2018). Structural Design and Manufacturing Process of a Low Scale Bio-Inspired Wind Turbine Blades.
- Ikeda, T., Tanaka, H., Yoshimura, R., Noda, R., Fujii, T., & Liu, H. (2018). A robust biomimetic blade design for micro wind turbines. *Renewable Energy*, 125, 155-165.
- Jaworski, J. W., & Peake, N. (2013). Aerodynamic noise from a poroelastic edge with implications for the silent flight of owls. *Journal of Fluid Mechanics*, 723, 456-479.
- Johansen, J., Sørensen, N. N. 2007. Numerical analysis of winglets on wind turbine blades using CFD. In *European Wind Energy Congress*. Milano: EWEA.
- Johari, H., Henoch, C., Custodio, D., & Levshin, A. (2007). Effects of leading-edge protuberances on airfoil performance. *AIAA journal*, 45(11), 2634-2642.
- Johnson, G. L. (1985). *Wind energy systems* (pp. 147-149). Englewood Cliffs, NJ: Prentice-Hall.
- Kalmikov, A. (2017). *Wind power fundamentals*. In *Wind Energy Engineering* (pp. 17-24). Academic Press.
- Külekcı, Ö. C. (2009). Yenilenebilir enerji kaynakları arasında jeotermal enerjinin yeri ve Türkiye açısından önemi. *Ankara Üniversitesi Çevre Bilimleri Dergisi*, 1(2), 83-91.
- Oerlemans, S., Fisher, M., Maeder, T., & Kögler, K. (2009). Reduction of wind turbine noise using optimized airfoils and trailing-edge serrations. *AIAA journal*, 47(6), 1470-1481.
- Özkaya, M., Variyenli, H., & Korkmaz, M. (2008). Rüzgar enerjisinden elektrik enerjisi üretimi ve Kayseri ili için çevresel etkilerinin değerlendirilmesi.
- Schubel, Peter J., and Richard J. Crossley. "Wind turbine blade design." *Energies* 5.9, 2012: 3425-3449.
- Seidel, C., Jayaram, S., Kunkel, L., & Mackowski, A. (2017). Structural analysis of biologically inspired small wind turbine blades. *International Journal of Mechanical and Materials Engineering*, 12(1), 1-9.
- Shi, W., Atlar, M., & Norman, R. (2017). Detailed flow measurement of the field around tidal turbines with and without biomimetic leading-edge tubercles. *Renewable Energy*, 111, 688-707.
- Uzun, M. & Çoban, S. (2021). Aerodynamic Performance Improvement with Morphing Winglet Design. *Journal of Aviation*, 5 (1), 16-21.
- Wright, G. (2017). *Bio-Inspired Wind Turbine Blade Profile Design* (Doctoral dissertation).
- Yılmaz, S., & Kalkan, D. K. (2017). Enerji güvenliği kavramı: 1973 petrol krizi ışığında bir tartışma. *Uluslararası Kriz ve Siyaset Araştırmaları Dergisi*, 1(3), 169-199.

Cite this article: Uzun, M., Özdemir, M., Yıldırım, Ç.V., Çoban, S. (2021). A Novel Biomimetic Wing Design and Optimizing Aerodynamic Performance. *Journal of Aviation*, 6(1), 12-25.



This is an open access article distributed under the terms of the Creative Commons Attribution 4.0 International License

Copyright © 2022 *Journal of Aviation* <https://javsci.com> - <http://dergipark.gov.tr/jav>